ELSEVIER

PII: S0032-3861(97)00580-6

Polymer Vol. 39 No. 12, pp. 2683–2692, 1998

0032-3861/98/\$19.00+0.00

Layer structures 12. Chiral sanidic polyesters derived from 2,5-bis(hexadecyloxy)terephthalic acid, 2,5-bis((*S*)-2-methylbutoxy)terephthalic acid and 4,4′-dihydroxybiphenyl

Hans R. Kricheldorf* and Dirk F. Wulff
Institut für Technische und Makromolekulare Chemie, Bundesstr. 45,
D-20146 Hamburg, Germany
(Received 20 May 1997; revised 8 July 1997)

Three homopolyesters were prepared by polycondensation of 4,4′-dihydroxybiphenyl and 2,5-bis(*n*-octyloxy)-, 2,5-bis(dodecyloxy)- or 2,5-(hexadecyloxy)terephthaloylchloride. Furthermore, several copolyesters were synthesized from 4,4′-dihydroxybiphenyl and mixtures of 2,5-bis(hexadecyloxy)terephthaloylchloride and 2,5-bis((*S*)isopentyloxy)terephthaloylchloride. All polyesters were characterized by inherent viscosities, elemental analyses, ^{1}H n.m.r. spectroscopy, d.s.c. measurements, dynamic mechanical analyses (DMA), WAXS powder patterns at various temperatures and optical microscopy. Two liquid crystalline (LC) phases were detected for the homopolyesters and most copolyesters: a viscous sanidic (biaxial nematic) phase and, at higher temperatures, a mobile nematic phase. The chiral copolyesters displayed an unusual ‘sausage texture’, but never a Grandjean texture. A chiral nematic phase with helical main chains is discussed. © 1998 Elsevier Science Ltd. All rights reserved.

(Keywords: chiral terephthalic acids; cholesteric polyesters; sanidic layers)

INTRODUCTION

Sanidic polyesters are polyesters forming a layered supramolecular structure with the layer planes parallel to the main chain[1] in contrast to the smectic systems where the layer planes are more or less perpendicular. Most sanidic polyesters studied so far are polyesters derived from terephthalic acid and alkyl-substituted hydroquinone (1)[2] or from substituted terephthalic acid and hydroquinone (2a,b)[3–9] or substituted hydroquinones[10]. Only quite recently sanidic polyesters derived from 4,4′-dihydroxybiphenyl and 2,5-bis(dodecyloxy)terephthalic acid (3b) were described and reported to form a honeycomb-like layer structure in the solid state[11,12]. The greater length of the biphenyl unit relative to hydroquinone and terephthalic acid has several interesting consequences. When compared to the analogous polyesters of hydroquinone 2a ($n = 11$), the phase transitions occur at lower temperatures, the dodecyl substituents do not crystallize and a broad nematic phase is formed. Furthermore, the sanidic layer structure may partially collapse to a honeycomb structure[11] which allows a denser packing of the alkyl side chains; which is not necessary in the case of the polyesters 2a. These properties render polyesters of structure 3 interesting substrates for the study of the influence of chiral centers on the phase behaviour and phase transitions.

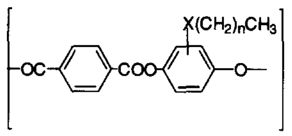

1

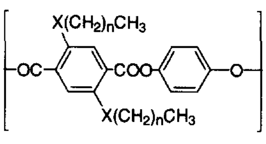

2a: X = O; 2b: X = S

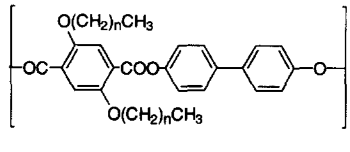

a: n = 7

b: n = 11

c: n =15

3a-c

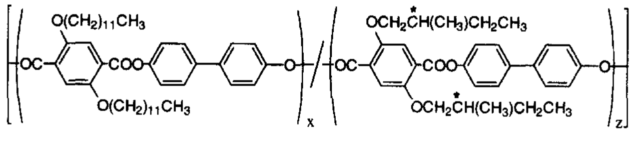

4a-f

a: x/z = 9/1
b: x/z = 8/2
c: x/z = 7/3
d: x/z = 5/5
e: x/z = 3/7
f: x/z = 0/10

In a previous part of this series[13], the copolyesters 4a–e and the homopolyester 4f having chiral centers in the side chains were described. Furthermore, copolyesters of the structure 5a–e were studied which possess a chiral unit in the main chain[14]. In the case of 4a–e only one chiral nematic phase was observed, whereas two LC phases were found in the case of 5a–e. In addition to a mobile cholesteric phase, a highly viscous sanidic liquid crystalline (LC) phase was detected at lower temperatures. In this connection the present work deals with the characterization of the homopolyesters 3a–c and of the chiral copolyesters 6a–d. The purpose of this work was two-fold. Firstly, the existence

---

*To whom correspondence should be addressed

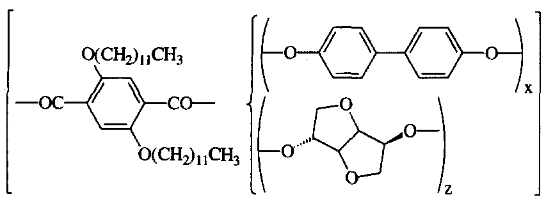

5a-e

a: x/z = 9.5/0.5
b: x/z = 9/1
c: x/z = 8/2
d: x/z = 7/3
e: x/z = 5/5

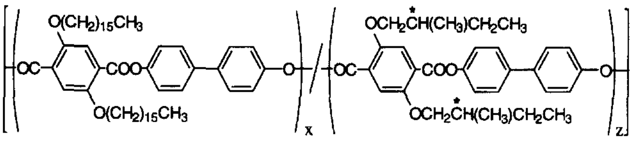

6a-e

a: x/z = 9/1
b: x/z = 8/2
c: x/z = 7/3
d: x/z = 5/5
e: x/z = 0/10

of a highly viscous sanidic LC phase should be confirmed for all these homo- and copolyesters. Secondly, the textures should be studied and compared to those of 4a–f and 5a–e. In the case of 5a–e normal cholesteric schlieren textures including a Grandjean (GJ) texture were found. In contrast, 4a–f did not form a GJ texture, but yielded an unusual texture labelled X or 'sausage texture'. This texture was related to an unusual chiral nematic phase based on twisted main chains. The properties of the copolyesters 6a–d were expected to confirm the experimental results and their interpretation reported for the copolyesters 4a–f. In this connection it should be emphasized that no low-molecular mass mesogens or LC side chain polymers can be synthesized which could serve as models of this special chiral nematic phase.

EXPERIMENTAL

Materials

Diethyl-2,5-dihydroxyterephthalate, *n*-octylbromide, *n*-dodecylbromide, *n*-hexadecylbromide, (*S*)-2-methylbutanol, tosylchloride and 4,4′-dihydroxybiphenyl were all purchased from Aldrich Co. (Milwaukee, WI, USA) and used as received. The chiral terephthalic acid and its dichloride (m.p. 51°C) was synthesized as described previously[15]. 2,5-Bis(octyloxy)terephthaloylchloride (m.p. 58°C), 2,5-bis-(dodecyloxy)terephthaloylchloride (m.p. 64°C), 2,5-bis(hexadecyloxy)-terephthaloylchloride (m.p. 75°C) were also prepared according to the literature[16]. 4,4′-Bistrimethylsiloxybiphenyl was obtained by silylation of 4,4′-dihydroxybiphenyl with an excess of hexamethyldisilazane in refluxing toluene (m.p. 64°C[17]).

Polycondensations

Silyl method. 4,4′-Bistrimethylsiloxybiphenyl (10 mmol), a substituted terephthaloylchloride (10 mmol) and benzyltriethylammonium chloride (10 mg) were weighed into a cylindrical glass reactor equipped with a mechanical stirrer, gas inlet and outlet tubes. The reaction vessel was placed into a metal bath preheated to 150°C. The reaction mixture was in the molten state at this temperature, and a slow evolution of chlorotrimethylsilane was observed. The temperature was raised in steps of 10°C per 10 min up to a final temperature of 260–280°C in order to keep the mixture in the molten state. Finally vacuum was applied for 15 min. The cold product was dissolved in a mixture of CH_2Cl_2 and trifluoroacetic acid (TFA) (volume ratio, 4:1) and precipitated into methanol. The isolated polyesters were dried at 80°C for 2 days in vacuo.

HCl method. 4,4′-Dihyroxybiphenyl (30 mmol) and a substituted terephthaloylchloride (30 mmol) were refluxed in dry diphenyl ether (100 mmol) with slow stirring. The liberated HCl was removed with a slow stream of nitrogen. When the evolution of HCl had nearly stopped, the cold reaction mixture was diluted with dichloroethane and precipitated into cold methanol. The isolated polyesters were dried at 120°C in vacuo.

Measurements

The inherent viscosities were measured with an Ubbelohde viscometer thermostated at 20°C (polyesters synthesized by the silyl method) or 25°C (polyesters synthesized by the HCl method).

The optical rotations were measured with a Perkin-Elmer M 241-in cuvette of 10 mm length.

The d.s.c. measurements were conducted with a Perkin-Elmer DSC 4 in aluminium pans under nitrogen.

The DMA measurements were conducted with a Du Pont DMA 983 in resonance with a sample size of 13 × 0.2 × 8 mm (*lwh*) and an amplitude of 0.3 mm.

The WAXS powder patterns were recorded either with a Siemens D-500 diffractometer using Ni-filtered Cu Kα radiation or by means of synchrotron radiation at HASYLAB (DESY, Hamburg, Germany). A one-dimensional position-sensitive detector was used at a heating rate of 10°C/min.

The ^{13}C n.m.r. CP/MAS spectra were recorded with a Bruker MSL 300 at 75.5 MHz in 7 mm ZrO_2 rotors:

Table 1 Yields and properties of polyesters 3a–c

Polymer (no.)	Synth. method[a]	Yield (%)	η_{inh} (dl/g)[b]	Elem. formula (form. weight)		Element analysis (%)	
						C	H
3a	B	81	3.24[c]	$C_{36}H_{44}O_6$ (572.75)	calc. found	75.50 74.85	7.74 7.67
3b′	A	95	0.54	$C_{44}H_{60}O_6$ (684.96)	calc. found	77.16 76.87	8.83 8.88
3b	B	85	1.90[c]	$C_{44}H_{60}O_6$ (684.96)	calc. found	77.16 77.37	8.83 8.89
3c′	A	85	0.27	$C_{52}H_{76}O_6$ (797.18)	calc. found	78.25 77.63	9.72 9.61
3c	B	99	3.45[c]	$C_{52}H_{76}O_6$ (797.18)	calc. found	78.25 78.30	9.72 9.41

[a] Method A, silyl method; method B, HCl method
[b] Measured at 20°C (method A) or 25°C (method B) with c = 2 g/l in CH_2Cl_2/TFA (volume ratio 4:1)
[c] Soluble fraction (90–95% of the total yield)

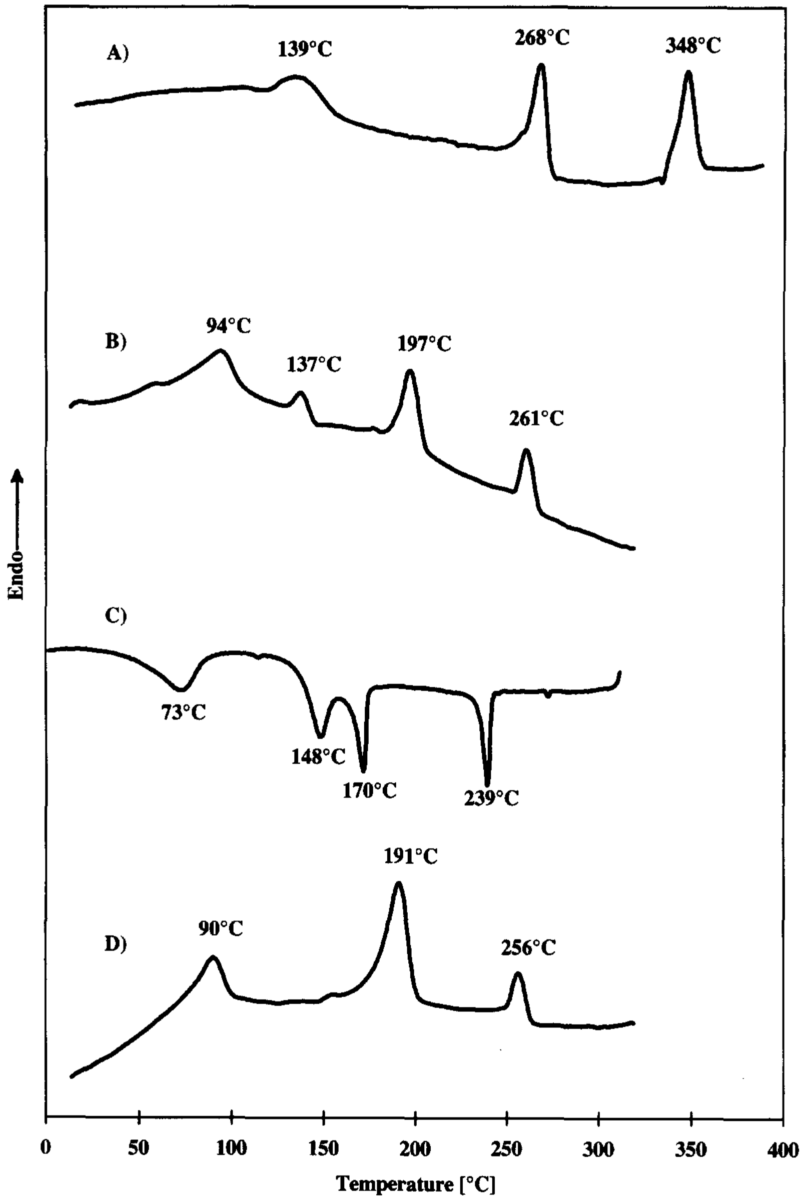

Figure 1 D.s.c. measurements (heating and cooling rate, 20°C/min): (A) first heating of homopolyester 3a; (B) first heating of homopolyester 3c; (C) first cooling of 3c; (D) second heating of 3c

spinning rate, 4 kHz; recycling delay, 4 s; and contact time, 1 ms.

RESULTS AND DISCUSSION

Homopolyesters 3a–c

In order to see if the properties of homopolyesters 3a–c are independent of the synthetic route, polyesters 3b and 3c were prepared by two different methods. For both methods the dichlorides of the substituted terephthalic acids were used. In the case of method A, the terephthaloyl dichlorides were polycondensed with the silylated 4,4′-dihydroxybiphenyl in bulk and chloride ions were used as catalysts. Characteristic for method B was the polycondensation of free 4,4′-dihydroxybiphenyl in a liquid inert reaction medium. For this purpose diphenyl ether was used in the present work. As demonstrated by the results listed in *Table 1* the 'HCl method' (B) gave higher viscosity values, whereas the yields and elemental analyses were satisfactory in all cases. The question why the 'silyl method' yielded relatively low viscosities in the present work was not investigated. In previous studies of other LC polyesters, higher viscosities were obtained with the 'silyl method'[18]. All the polyesters from the 'HCl method' (B) contained a small fraction of insoluble gel particles indicating that the liberated HCl had caused side reactions resulting in branching and crosslinking (presumably via ether linkages). These side reactions explain, at least partially, why higher viscosity values were obtained. In order to avoid such side reactions of the possibly more acid-sensitive chiral substituent, all the chiral polyesters were prepared by the silyl method.

The thermal properties of polyester 3b (and 3b′) have been discussed in previous papers[13,14]. It was found that the d.s.c. heating curves display a weak endotherm in the temperature range of 90–110°C (depending on the molecular weight) which was poorly reproducible in the second heating trace. Only by DMA measurements was a transition from the solid to the liquid sanidic phase detected. The d.s.c. measurements of polyesters 3a and 3c (or 3c′) were more informative, as illustrated by *Figure 1*. Not only the first but also the second heating curves exhibited three endotherms.

In the case of 3c, even four endotherms appeared in the first heating curve, but only three of them were reproducible in the second and third heating traces. Therefore, these d.s.c. measurements of 3a, 3c and 3c′ definitely prove that the polyesters of structure 3 possess three first-order phase transitions labeled T_{m1}, T_{m2} and T_i in *Table 2*). The temperatures of these transitions depend on the molecular weight as discussed previously for 3b and 3b′ and again demonstrated for 3c and 3c′ in this work (*Table 2*). Furthermore, the temperatures of all three phase transitions increase with decreasing lengths of the alkyl side chain.

The first phase transition (T_{m1}) represents the change from a solid sanidic phase to a sanidic LC phase. This interpretation is based on DMA measurements which show that the homopolyesters began to flow above T_{m1} (*Figure 2*). Secondly the X-ray measurements with synchrotron radiation revealed that the middle angle reflections (MARs) indicating the *d*-spacing of the layer structure vanish at T_{m2}

Table 2 Thermal properties of polyesters 3c, 3c′ and 6a–e

Polymer (no.)		T_G (°C)[c]	T_{m1} (°C)[c]	T_{m2} (°C)[c]	T_i/T_{ai} (°C)[c]	T_i (°C)[d]	T_{ai} (°C)[d]
3c′[a]	1st heat	—	107	—	180	190–208	196–189
	1st cool	—	—	—	164	—	—
	2nd heat	—	112	—	185	—	—
3c[b]	1st heat	—	—	197	261	261–266	250
	1st cool	—	—	170	239	—	—
	2nd heat	—	—	191	256	—	—
6a	1st heat	—	109	156	200	—	—
	1st cool	—	—	135	192	208–216	208–204
	2nd heat	—	110	156	199	—	—
6b	1st heat	—	—	165	211	224–232	224–219
	1st cool	—	—	140	206	—	—
	2nd heat	—	—	157	211	—	—
6c	1st heat	—	132	165	213	215–227	221–215
	1st cool	104	—	142	207	—	—
	2nd heat	106	130	160	215	—	—
6d	1st heat	—	—	171	247	250–255	249–241
	1st cool	—	—	158	—	—	—
	2nd heat	—	—	179	—	—	—
6e	1st heat	—	—	378	—	—	—
	1st cool	—	—	(dec.)	dec.	dec.	dec.
	2nd heat	—	—	—	—	—	—

[a] Silyl method (A)

[b] HCl method (B)

[c] From d.s.c. measurements with a heating (cooling) rate of 20°C/min

[d] From optical microscopy with a heating (cooling) rate of 20°C/min

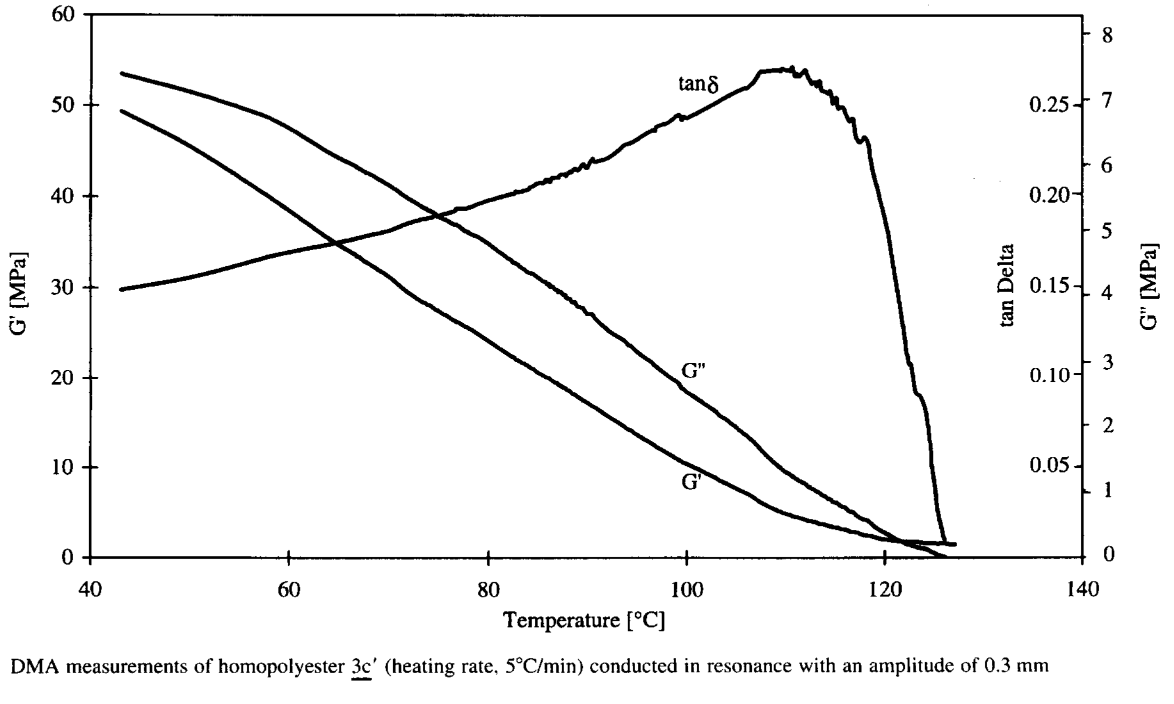

Figure 2 DMA measurements of homopolyester 3c′ (heating rate, 5°C/min) conducted in resonance with an amplitude of 0.3 mm

and not at T_{m1} (see Ref. [9] and discussion below). Thirdly, optical microscopy with crossed polarizers of the low-molecular weight samples 3b′ and 3c′ revealed that the phase between T_{m1} and T_{m2} is mobile under slight pressure, although this phase is highly viscous. For such microscopic observations it is an advantage to have samples of relatively low molecular weight available, because the higher melt viscosity of samples 3a, 3b and 3c did not allow the detection of a mobile phase between T_{m1} and T_{m2}.

The textures characteristic for the homopolyesters of structure 3 are illustrated in *Figure 3*. The sanidic LC phase displays a somewhat diffuse schlieren texture (*Figure 3A*), whereas above T_{m2} a normal nematic schlieren texture is found which forms broader schlieren upon increasing temperature (*Figure 3B* and *Figure 3C*).

The WAXS powder patterns of 3a–c allow a calculation of the *d*-spacings of the layer structures from the MARs via the Bragg equation (*Figure 4*). These *d*-spacings indicate that the sanidic layers of 3a–c are formed by interdigitating of almost fully extended side chains (see Ref. [9]). The *d*-spacings increase with the length of the alkyl side chains from 18 (3a) to 23 (3b) and 28 Å (3c). This increase corresponds to an increment of 1.25 Å per methylene group, which is close to the value of 1.27 Å typical of a fully extended alkyl chain in the all-*trans* conformation. However, it should be emphasized that neither the d.s.c. measurement nor the WAXS powder pattern gave any indication for a crystallization of the alkyl side chains, as was observed for the polyesters of structure 2. The greater length of the biphenyl units compared to hydroquinone

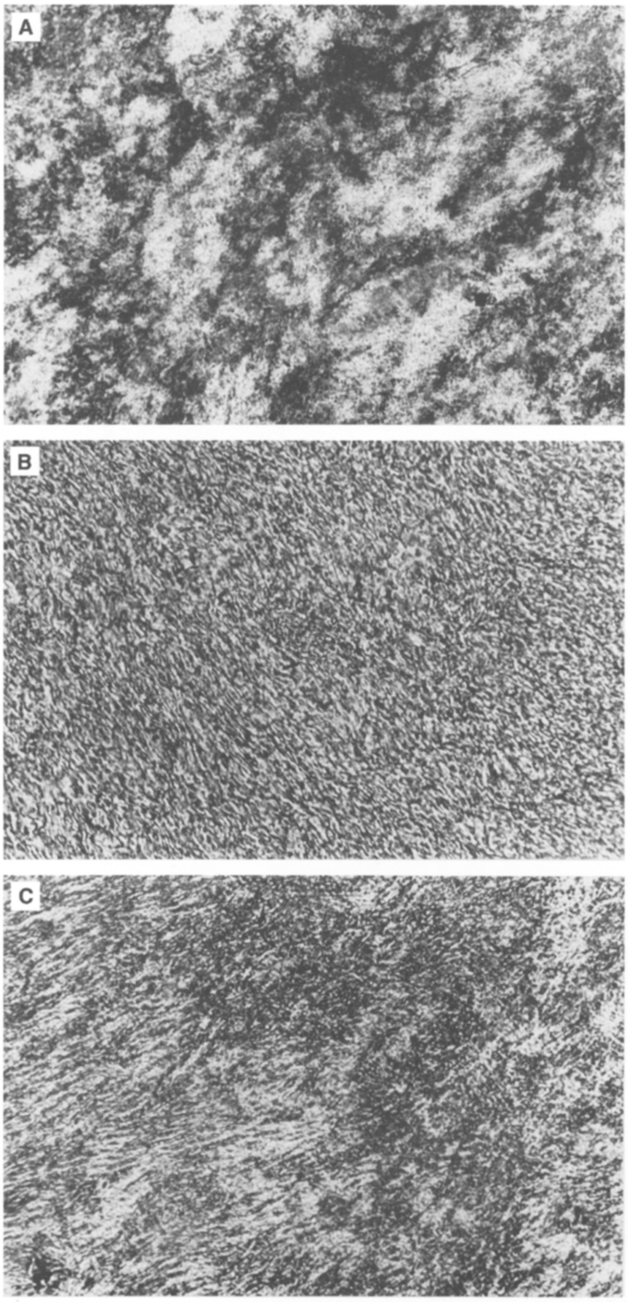

Figure 3 Textures (magnification 360 ×) of homopolyester 3c: (A) at 180°C; (B) at 205°C; (C) at 245°C

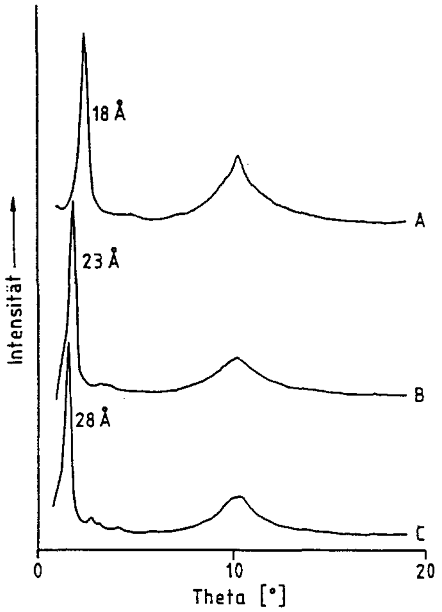

Figure 4 WAXS powder patterns of homopolyesters (A) 3a, (B) 3b, and (C) 3c

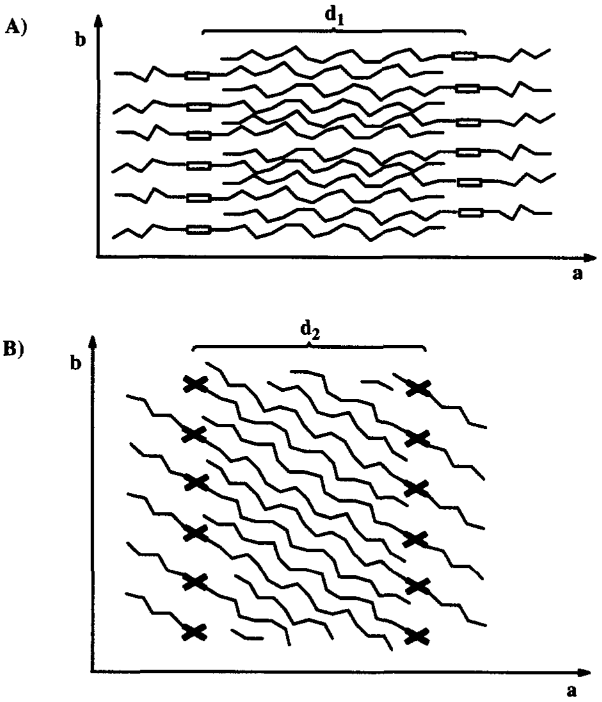

Figure 5 Schemes of two different kinds of sanidic layer structures

prevents the dense packing of the side chains required for crystallization.

Another interesting result of the present study is the finding that the *d*-spacings of sample 3c′ (prepared by the silyl method) amounts to only 24 Å. This value is not a mistake or irreproducible, because nearly the same value was found for all copolyesters 6a–d when quenched from the isotropic melt. Molecular modelling indicates that the long biphenyl units offer enough space for a back-folding (hair-pin conformation) of the alkyl side chains. An alternative explanation is the assumption of a tilted array of the alkyl side chains (*Figure 5B*) in contrast to the perpendicular array illustrated by *Figure 5A*. A tilted sanidic phase was also discussed for the analogous homopolyesters

Table 3 Yields and properties of polyesters 6a–d prepared by method A

Polymer (no.)	Yield (%)	η_{inh} (dl/g)[b]	$[\alpha]_{20}^{D}$ (°)[b]	Elem. formula (form. weight)	Element analysis (%)		
						C	H
6a	89	0.45	0	$C_{498}H_{716}O_{60}$ (7663.206)	calc. found	78.05 77.81	9.42 9.24
6b	93	0.49	+ 2	$C_{476}H_{672}O_{60}$ (7354.61)	calc. found	77.74 75.56	9.21 8.62
6c	96	0.47	+ 3	$C_{454}H_{628}O_{60}$ (7046.02)	calc. found	77.39 76.26	8.98 8.77
6d	96	0.54	+ 5	$C_{82}H_{108}O_{12}$ (1285.77)	calc. found	76.60 75.82	8.47 8.17
6e	96	0.78	+ 10	$C_{30}H_{23}O_6$ (479.51)	calc. found	75.14 73.28	4.83 6.55

[a] Measured at 20°C with $c = 2$ g/l in CH_2Cl_2/TFA (volume ratio, 4:1)
[b] Measured at 20°C with $c = 2$ g/l in CH_2Cl_2/TFA (volume ratio 7:1), $\lambda = 546$ nm

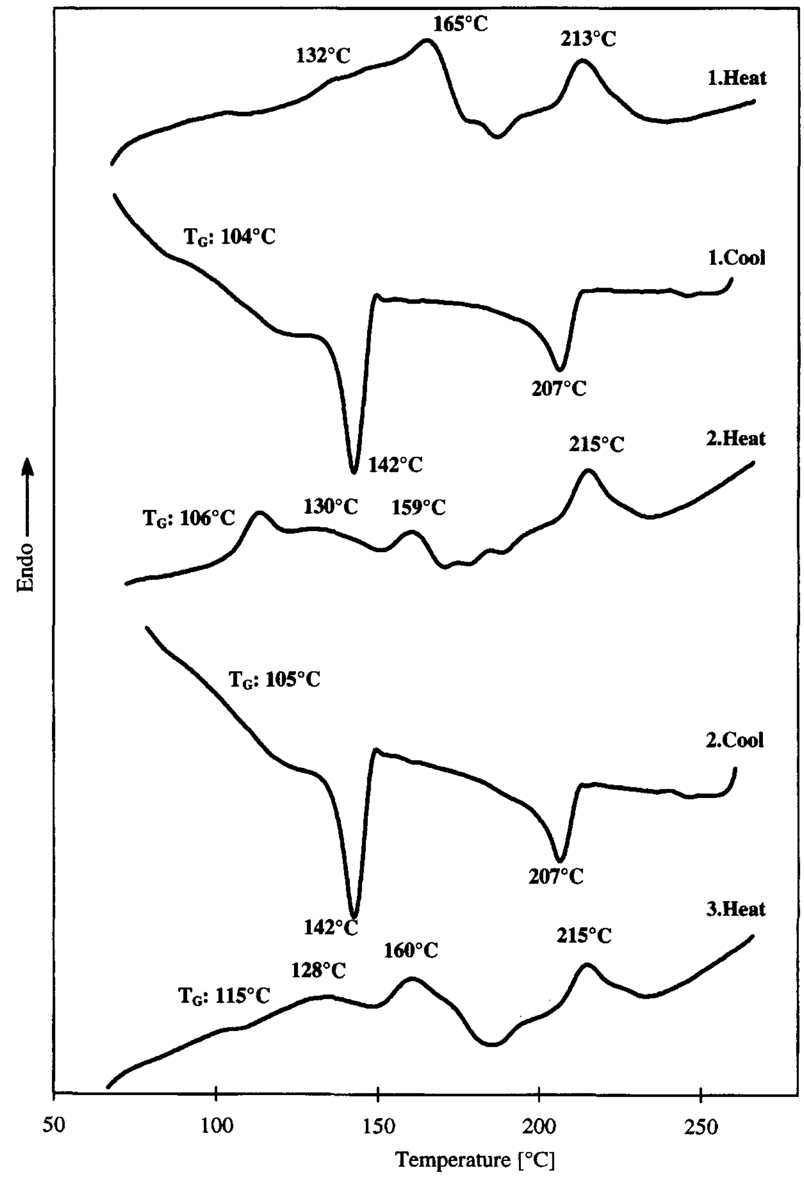

Figure 6 D.s.c. measurements of copolyester 6c with a heating and cooling rate of 20°C/min

of hydroquinone (2a)[6]. However, in that case the alkyl side chains form crystalline paraffin domains which stabilize the sanidic phase. In contrast, the alkyl side chains of 3b or 3c (and 3c′) do not crystallize and are more mobile. This conclusion is evident from the absence of 'paraffin reflections' in the WAXS powder patterns and the absence of endotherms and exotherms in the d.s.c. curves, indicating a reversible melting of ordered paraffin domains. Finally, ^{13}C n.m.r. CP/MAS spectra were recorded of 3c, and 3c′ at 25°C, to find out if their side chain conformations are different in relation to the different *d*-spacings. However, in both cases a strong signal at 31 ppm was found representing gt conformations. The signals of tt conformation at 33–34 ppm and of gg conformation at 27–28 ppm were weak (about 15% of the gt signal). These n.m.r. measurements exclude the existence of ordered paraffin domains based on alkyl chains in the all-*trans* conformation. Furthermore, the n.m.r. measurements did not reveal any conformational difference between 3c and 3c′. Therefore, no decision can be made at this time as to which hypothesis is the correct explanation of the different *d*-spacings.

Copolyesters 6a–d

Copolyesters 6a–d and the chiral homopolyester 6e were all prepared via the silyl method (A) in bulk. High yields and moderate inherent viscosities were obtained (*Table 3*). The optical rotations increase parallel to the feed ratio of the chiral terephthalic acid. These optical rotations, the elemental analyses and the ^{1}H n.m.r. spectra proved the structure of these polyesters.

The d.s.c. measurements of polyesters 6a–c showed a pattern of phase transitions quite analogous to those of homopolyesters 3a′. Three endotherms were observable in the heating curves, but only two exotherms appeared in the cooling curves, as illustrated exemplarily for 6c in *Figure 6*. The first transition was not detectable in the d.s.c. curves of 6d, whereas the endotherms of T_{m2} and of the isotropization were still observable. The chiral homopolyester possesses only one melting endotherm and does not form a LC phase. It decomposes immediately above its melting temperature.

The synchrotron radiation measurements of the middle angle reflection (MAR) yielded three interesting results (*Figures 7 and 8*). Firstly, the melting process at T_{m1} is

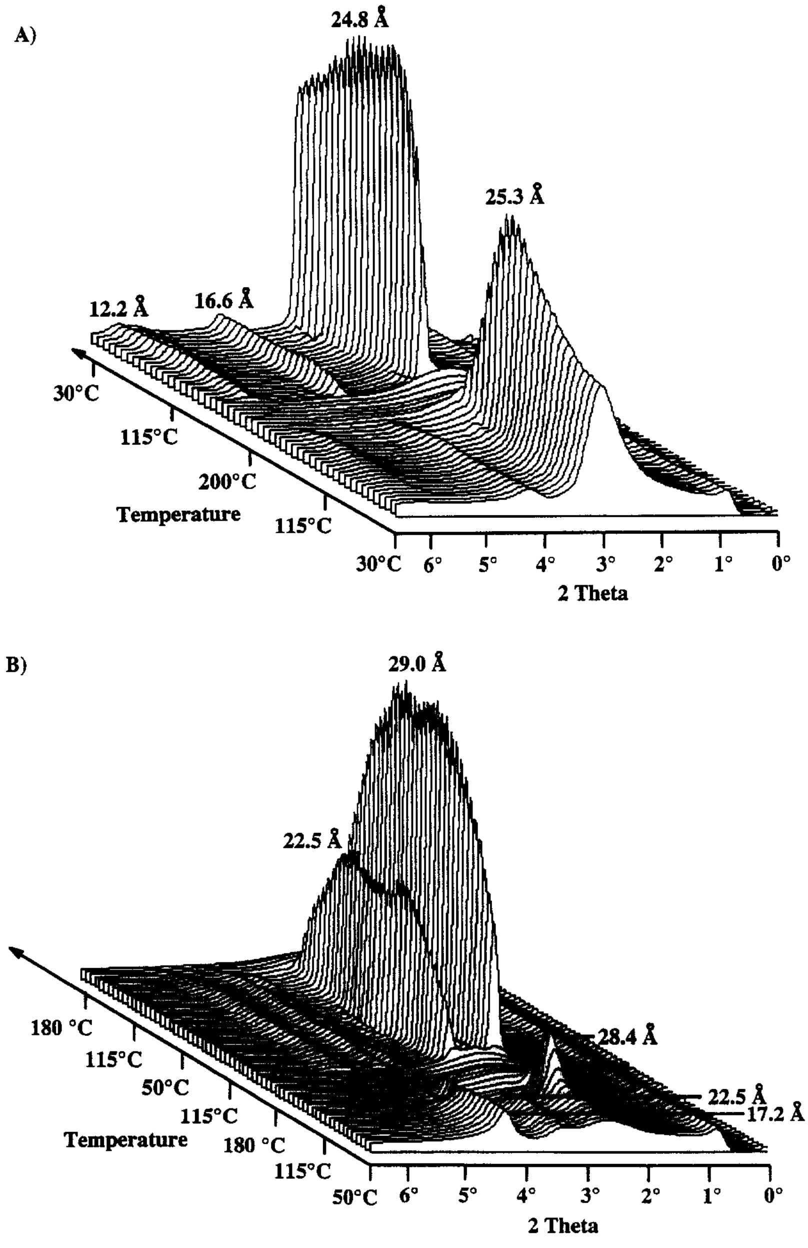

Figure 7 Middle angle measurements of (A) homopolyester 3c′ and (B) copolyester 6b, conducted with synchrotron radiation at a heating and cooling rate of 10°C/min

detectable by a change of the intensity of the MARs. Secondly, the MARs vanish completely at T_{m2} proving that the LC phase between T_{m1} and T_{m2} is a sanidic (or in other words biaxial nematic) phase. Thirdly, the MARs of copolyester 6b show a complexity not observed for the other copolyesters (*Figure 7*). Three MARs appear in the first heating curve, but only two of them are reproducible in the cooling and second heating curve. A straightforward explanation of this phenomena cannot be offered at this time, in as much as 6a and 6c (the neighbouring copolyesters) show a normal behaviour with only one reproducible MAR. Another, somewhat surprising finding concerns the layer distance (*d*-spacing) calculated for 6a–d. It was found for the analogous copolyesters 4a–e that the layer distance shrinks when the molar fraction of the chiral terephthaloyl unit increases, because its substituents need less space. This tendency was not observed for 6a–d. When copolyesters 6a–d were quenched from the isotropic melt, their X-ray measurements showed MARs in the range of 23–24 Å. This value agrees well with that of the homopolyester 3c′. When the copolyesters were annealed at 200°C for 1 h the MAR of 6d remained almost unchanged. In the case of 6a–c, MARs in the range of 27.5–28.5 Å were found corresponding to the *d*-spacing of homopolyester 3c (*Figure 9*). These results demonstrate that it is mainly the thermal history, and not so much the content of the chiral substituent, which influences the *d*-spacing.

Examination by optical microscopy with crossed polarizers gave the following results. For the sanidic LC phase between T_{m1} and T_{m2} colourful broad schlieren textures were observed, and were quite similar to those of homopolyesters 3a–c (*Figure 3A*). Another type of mobile schlieren texture was observed above T_{m2}. Quite analogous to the optical properties of 4a–e, no Grandjean texture was obtained by shearing of the chiral nematic phase regardless of the temperature and the composition. Furthermore, the 'sausage texture' (or texture X) reported as a typical feature of copolyester 4a–e was also obtained in the case of 6a–d

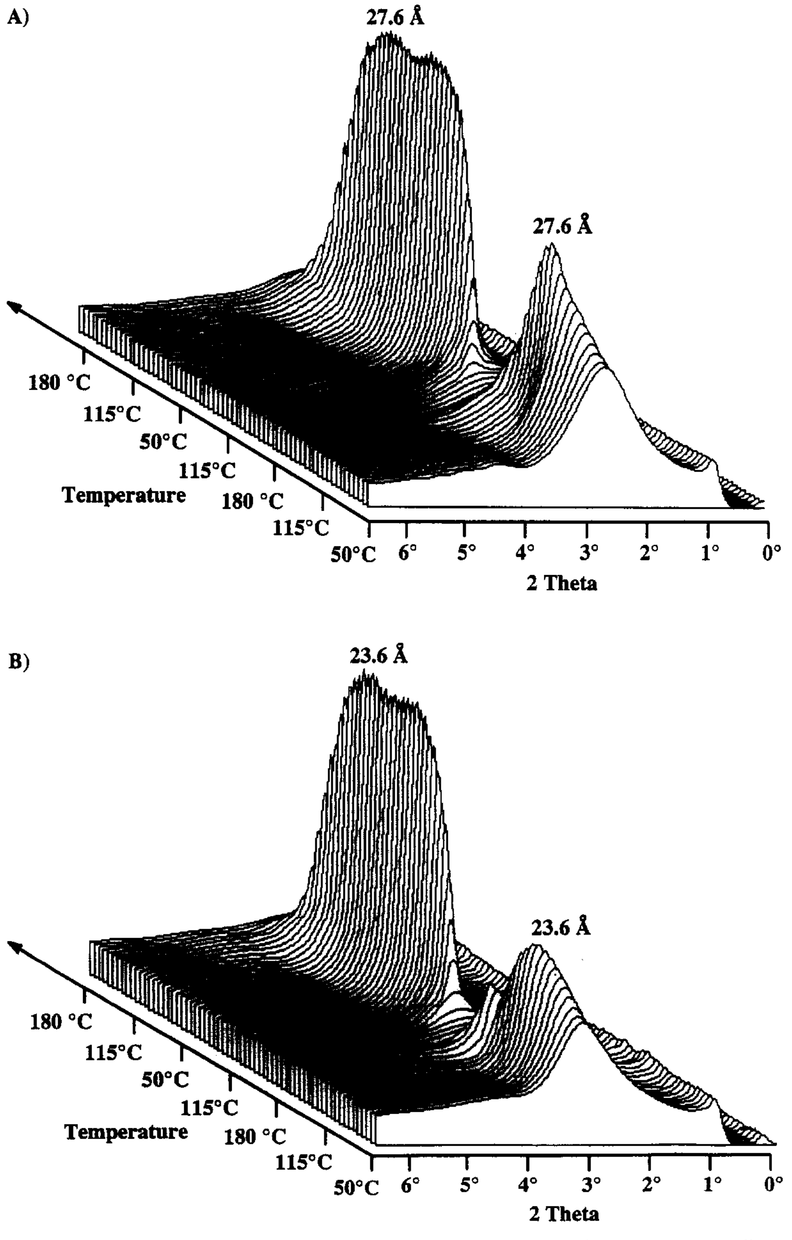

Figure 8 Middle angle measurements of (A) copolyester 6c and (B) copolyester 6d conducted with synchrotron radiation at a heating and cooling rate of 10°C/min

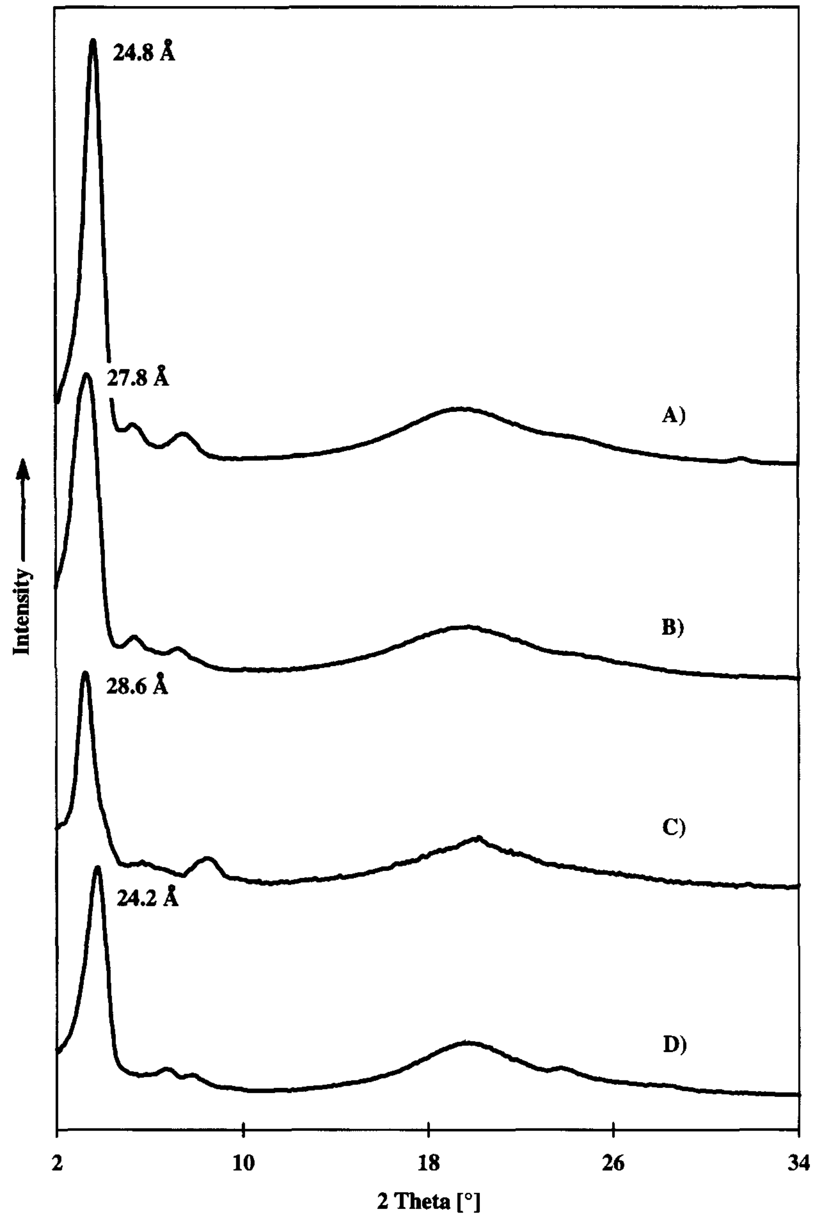

Figure 9 WAXS powder patterns: (A) of homopolyester 3c′, (B) of copolyester 6a, (C) of 6b, (D) of 6d

(*Figure 10*). It is characteristic for this texture that it is only black and white, although the microscope condition allows the observation of colours. These optical properties of 6a–d or 4a–f represent an important difference from those of 5a–d. Copolyester 5b was found to form a Grandjean texture, whereas none of the copolyesters containing isosorbide showed the 'sausage texture'. The similarity between 4a–f and 6a–d on the one hand, and the difference to 5a–d on the other, supports our hypothesis that the chiral nematic phase of the former polyesters contain helically twisted main chains (*Figure 11A*). They are too rigid to form the helical array of mesogenic groups or segments typical of a normal cholesteric phase (*Figure 11B*). In the case of 5a–d, the isosorbide induces bends and hair-pin conformations which allow the formation of a normal cholesteric order.

CONCLUSIONS

The results of the present work allow several interesting conclusions. Both homopolyesters 3a–c and chiral copolyesters 4a–f or 6a–d show three first-order phase

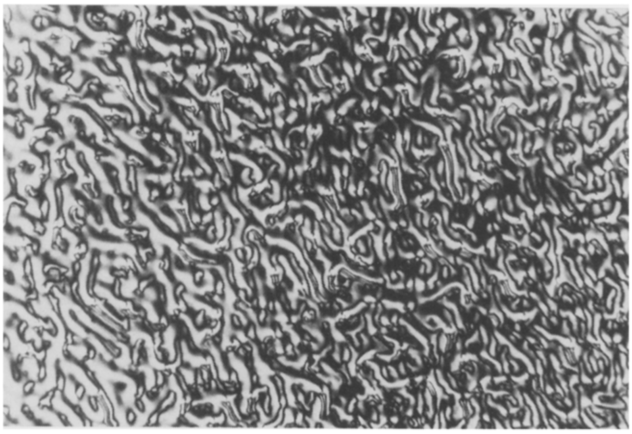

Figure 10 Texture (magnification 360 ×) of copolyester 6b at 220°C

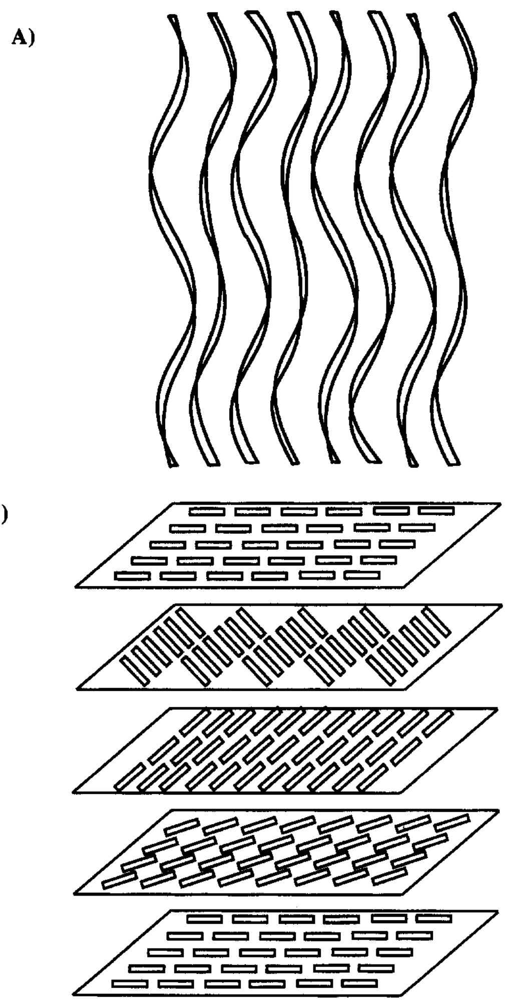

Figure 11 (A) Scheme of twisted chains in the chiral nematic melt (above T_{m2}) Of copolyesters 6a–d; (B) scheme of a cholesteric order of mesogenic groups

transitions. The first transition (T_{m1} in the range of 80–140°C) represents the melting of a solid sanidic phase into a sanidic LC phase having the same *d*-spacing. This highly viscous phase may also be labeled biaxial nematic phase in contrast to the normal monoaxially ordered nematic phase formed above T_{m2} (in the range of 160–220°C). The third transition (220–320°C) is the isotropization.

The optical properties of 6a–d proved to be nearly identical to those of 4a–e but different from those of 5a–d. Copolyesters 6a–d do not form a Grandjean texture but yield the unusual 'sausage texture' that has never been observed in the case of 5a–d. This characteristic difference may be a consequence of different main chain conformations.

ACKNOWLEDGEMENTS

We wish to thank the Deutsche Forschungsgesellschaft for financial support.

REFERENCES

1. Herrmann-Schönherr, O., Wendorff, J., Ringsdorf, H. and Tschirner, P., *Makromol. Rapid Commun.*, 1987, **7**, 791.
2. Fujishiro, K. and Lenz, R.W., *Macromolecules*, 1992, **25**, 81.
3. Ballauff, M., *Makromol. Chem. Rapid Commun.*, 1986, **7**, 407.
4. Ballauff, M. and Schmidt, G.F., *Makromol. Chem. Rapid Commun.*, 1987, **8**, 93.
5. Falk, U. and Spiess, H.W., *Makromol. Chem. Rapid Commun.*, 1989, **10**, 149.
6. Adam, A. and Spiess, H.W., *Makromol. Chem. Rapid Commun.*, 1990, **11**, 249.
7. Berger, K. and Ballauff, M., *Mol. Cryst. Liq. Cryst.*, 1987, **147**, 163.
8. Clauss, J., Schmidt-Rohr, K., Adam, A., Boeffel, C. and Spress, W., *Macromolecules*, 1992, **25**, 5203.
9. Kricheldorf, H.R. and Domschke, A., *Macromolecules*, 1996, **29**, 1337.
10. Heitz, W., *Makromol. Chem. Macromol. Symp.*, 1991, **47**, 111.
11. Watanabe, J., Sekine, N., Nematsu, T., Sone, M. and Kricheldorf, H.R., *Macromolecules*, 1996, **29**, 4816.
12. Harkness, B.R. and Watanabe, J., *Macromolecules*, 1991, **24**, 6759.
13. Kricheldorf, H.R. and Wulff, D.F., *J. Polym. Sci. Part A. Polym. Chem.*, 1997, **35**, 947.
14. Kricheldorf, H. R. and Wulff, D. F., *Polymer*, in press (**proceeding part of this paper**).
15. Kricheldorf, H.R. and Wulff, D.F., *J. Polym. Sci. Part A Polym. Chem.*, 1996, **34**, 3511.
16. Kricheldorf, H.R., Weegen-Schulz, B. and Engelhardt, J., *Makromol. Chem.*, 1991, **192**, 631.
17. Stanley, H., Connel, S. and Winder, J., *J. Org. Chem.*, 1958, **23**, 50.
18. Kricheldorf, H.R., Engelhardt, J. and Weegen-Schulz, B., *Makromol. Chem.*, 1991, **192**, 645.